Stochastic acceleration of relativistic electrons and plasma heating and current drive with 2.45 GHz frequency at the WEGA stellarator

H P Laqua[1], E Chlechowitz[2], M Otte[1] and T Stange[1].

[1]Max Planck Institute for Plasma Physics, EURATOM Association, 17491 Greifswald, Germany

[2]HSX Plasma Laboratory, University of Wisconsin, Madison, USA

Laqua @ ipp.mpg,de

Abstract: MeV electrons were produced with less than 6 kW of non-resonant 2.45 GHz microwave heating at magnetic fields of 0.3-0.5 T with no applied loop voltage at the WEGA stellarator. The maximum toroidal plasma current, carried by the electrons, was 1 kA. Broadband radiation, similar to synchrotron radiation, was measured in the 0.5-120 GHz range. X-ray radiation from the plasma and directed γ-ray emission from collisions of the electrons with nearby plasma facing components was measured as well. The acceleration process was modeled by a tail formation due to stochastic interaction with the RF-field at the antenna mouth. The characteristic time for tail formation could be reproduced with power modulation experiments.

1. Introduction

A toroidal magnetic configuration with helically twisted magnetic field lines is able to perfectly confine ionized energetic particles with momentum, $mv_{||}$, parallel to the magnetic field. In a stellarator this configuration is established solely through the use of external coils. As long as the centrifugal force F_{cf} is negligible with respect to the radial magnetic field force F_m ($mv_{||}^2/R << qv_{||}B_\theta$), the particle orbits remain on the magnetic flux surfaces. Here R represents the radial position, q the charge and B_θ the poloidal component of the magnetic field, which generates the rotational transform of the field lines. For higher parallel momentum the particle orbits deviate from flux surfaces, but form their own closed drift surfaces. In the case that F_{cf} points in the same direction as F_m, the drift surfaces are larger than the flux surfaces and the orbits can exceed the confinement region and the particles may be lost by collision with the vacuum vessel. When F_m acts counter to F_{cf} the drift surfaces are displaced towards the torus outboard side but also shrink in radius with increasing parallel momentum as shown in **figure 1**. The orbits can even collapse to a point in the poloidal projection, the so called stagnation orbit with a maximum energy of up to 5 MeV for our experimental parameter, but are still stable [1]. More interesting for heating application are orbits which exceed the plasma edge and cross the axis of the bulk plasma as they can transfer energy into the plasma from outside of the last closed flux surface. The unidirectional confinement of the "runaway" orbits generates a net toroidal current. These orbits are easily achieved for electrons in tokamaks when a loop voltage is applied and plasma conditions allow the generation of runaway electrons. In stellarators a loop voltage is no longer necessary but would generate the same runaway electron population if applied [2]. This article reports the stationary generation of a runaway electron current by radio frequency heating with 2.45 GHz microwaves and bulk plasma heating by those electrons. The acceleration process is purely stochastic without any resonance between RF and particle motion. In contrast to the loop voltage generated runaway electrons, which are preferably generated in the plasma center, here the runaway electrons originate from the plasma edge close to the rf-antenna as shown in **figure 1**.

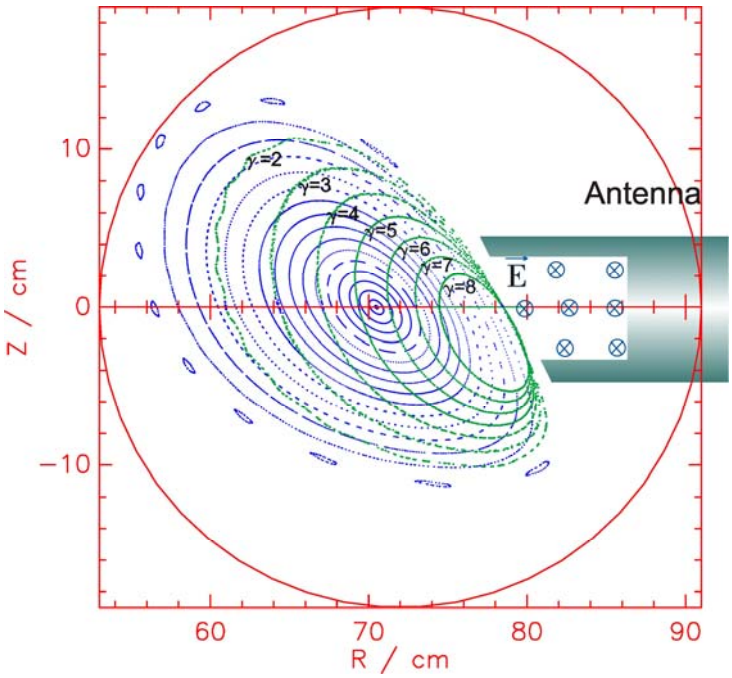

Figure. 1: Flux surfaces (blue) and particle drift surfaces (green) for different relativistic γ-factors. On the left there is a simplified sketch of the antenna field. This is a poloidal cut of a toroidal configuration.

2. Experimental set-up

WEGA is a classical five period and $l = 2$ stellarator with a major radius of 0.72 m and an aspect ratio of 7. It is equipped with the toroidal field coils and the two oppositely energized helical field coils that generate the rotational transform and thus the closed magnetic flux surfaces. The discharge length at 0.5 T is up to 20 s, which allows operating the plasma in a stationary state. WEGA is equipped with an electron cyclotron resonance heating (ECRH) system at a frequency of 28 GHz and with 10 kW (cw) power. The ECRH is supported by a 20 kW (cw) non-resonant 2.45GHz microwave system with a TE11 waveguide antenna with a diameter of 89 mm and a double cut at its front as described in [3]. This antenna generates an electric field of up to 100 kV/m with a polarization parallel to the magnetic field lines. The shape of the electric field pattern is assumed to be Gaussian with a 1/e half width of typically 30 mm. The antenna $N_{||}$ spectrum ($N_{||}<1$) is not appropriate to excite any plasma wave (lower hybrid type) efficiently, but the electric field can penetrate within its skin depth of about 1 mm into the plasma edge. WEGA is equipped with a central line of sight 80 GHz interferometer for time-resolved integrated density measurement. The density profile and the bulk electron temperature were measured by a movable Langmuir probe, which of course could perturb the plasma parameter. Thus the probe measurements give only a lower limit of the density and temperature. The plasma current was measured by a Rogowski coil outside of the vacuum vessel, which caused a delay of about 0.3 ms due to the flux penetration through the wall. The supra-thermal electrons are measured by their soft X-ray (sX) emission and γ-ray emission. The sX-diagnostic uses a Si(Li)-detector with a pulse height analyzer (PHA) allowing an energy resolution of at least 1keV up to a detection limit of around 200 keV. Dependant on the sight area of the detector one spectrum can be measured per shot. Their time dependence can be verified by a partially energy integrated count detection with a time resolution of at least 100 ms.

The γ-ray emission was measured with a Geiger-Müller-type detector (Gamma-Scout™) using the lead filter method. The detector was screened by a 100 mm thick lead tube with different lead foils at its front, pointing towards the source of highest emission. The microwave emission is detected by a 12 channel calibrated radiometer with a spectral range between 22 and 40 GHz. An additional measurement by a single frequency, un-calibrated Tektronix 2784 Spectrum Analyzer with external front-end mixer at frequencies up to 120 GHz was also used.

3. Heating scenario

The plasma was initiated by 28 GHz ECRH at a magnetic flux density B_0 on axis of 0.5 T. In most of the experiments the plasma working gas was helium, but experiments in hydrogen showed similar results. The plasma density was of the order of $1\text{-}2\times10^{18}$ m^{-3}, which was controlled through the neutral gas pressure. Once the plasma was established, the 2.45 GHz non-resonant heating was applied additionally. With increasing power a toroidal current of several hundred Amps was established, accompanied by a broadband radiation similar to synchrotron radiation with an observed radiation temperature of up to 1keV, continuous soft-X-ray emission with energies up to the detection limit of 200 keV and the emission of γ-radiation. The last prevented operation at power higher than 6 kW due to safety restrictions, due to insufficient screening. Once the 2.45 GHz heating power had reached flat top, the ECRH was switched-off and the stationary plasma was sustained solely by the 2.45 GHz microwave power for several seconds as shown in **figure 2**. B_0 could then be varied over a wide range (0.2- 0.5T) and was limited only by technical restrictions. The heating scenario was very robust and rather insensitive with respect to the antenna position and edge density. It has been operated at neutral He and hydrogen densities of $1\text{-}6\times10^{-5}$ mbar.

4. Experimental results

The synchrotron spectrum decreases with frequency. The spectral decay in **figure 3** fits well to the calculated one [4] for an electron energy between 2 and 2.5 MeV. The synchrotron emission intensity strongly increases with the particle energy and thus is indicative of the fastest electron component.
The observed γ-ray emission was inhomogeneous and anisotropic and its source was localized at the position of the ECRH launching mirror, which is the closest plasma facing component on the low-field side. Additionally, the γ-rays are emitted in the direction of the electron motion. When the magnetic field was reversed, the current also reversed and the γ-ray emission dropped by a factor 9 as shown in **figure 4**. Using different lead foils in front of the detector and taking into account the damping of the stainless steel vacuum chamber wall and the cooper cois, which were in the line of sight, the γ-ray intensity would represent a Bremstrahlung spectrum of a 600 keV mono-energetic beam.

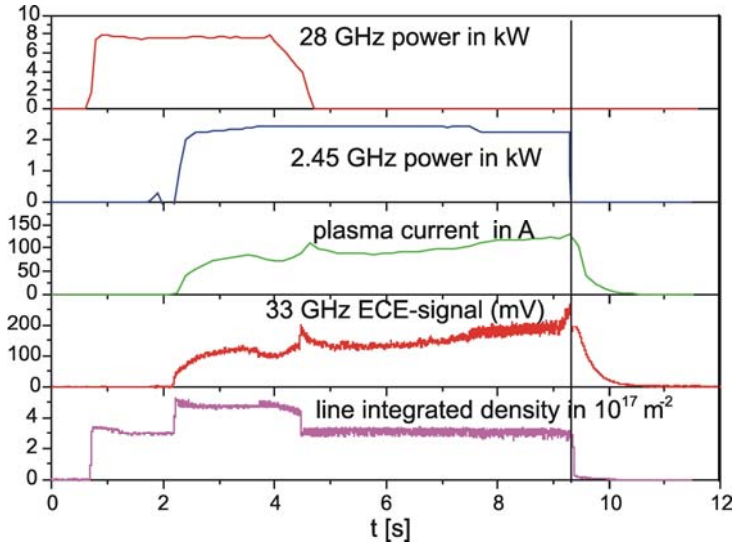

Figure 2: Heating scenario: Start-up with 28GHz ECRH at 0.5T up to t = 4.5 s. Pure non-resonant 2.45 GHz heating and current drive is established up to 9.3 s. Thereafter an exponential decay is seen in the plasma current and synchrotron radiation.

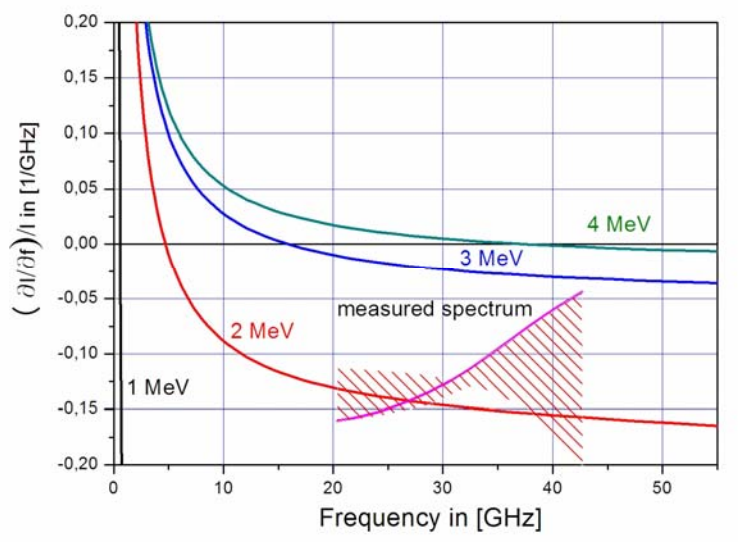

Figure 3: Calculated [4] (bending radius 0.74 m) and measured synchrotron spectral decay $(\partial I_{sync}/\partial f)/I_{sync}$ with error range, where *f* represents the frequency. The dashed area represents the error bars.

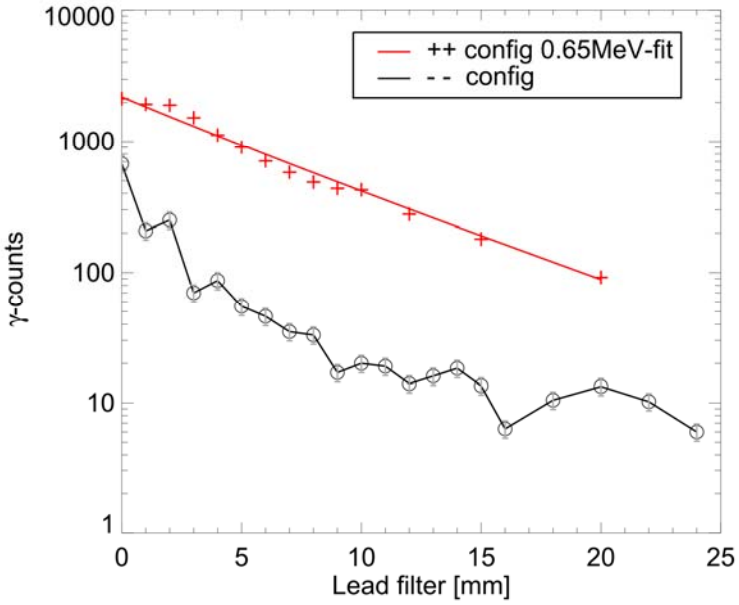

Figure 4: γ-ray intensity as a function of the lead filter thickness in front of the "Gamma Scout®" for co- and counter direction of the relativistic electron propagation.

The reversal of the plasma current and γ-ray emission direction proves the existence of relativistic electrons which are only confined for motion along one direction – as mentioned in the introduction. Their orbits are located at the plasma edge on the low field side, where a probe, moving radially into the plasma, collected the fast electrons. When it reached the plasma edge the plasma current, the synchrotron radiation and the soft-X-ray emission declined and vanished within the following 20 mm of probe motion as shown in **figure 5**. When the probe was removed the supra-thermal feature recovered as the bulk plasma in this experiment was still maintained by the 28 GHz ECRH.

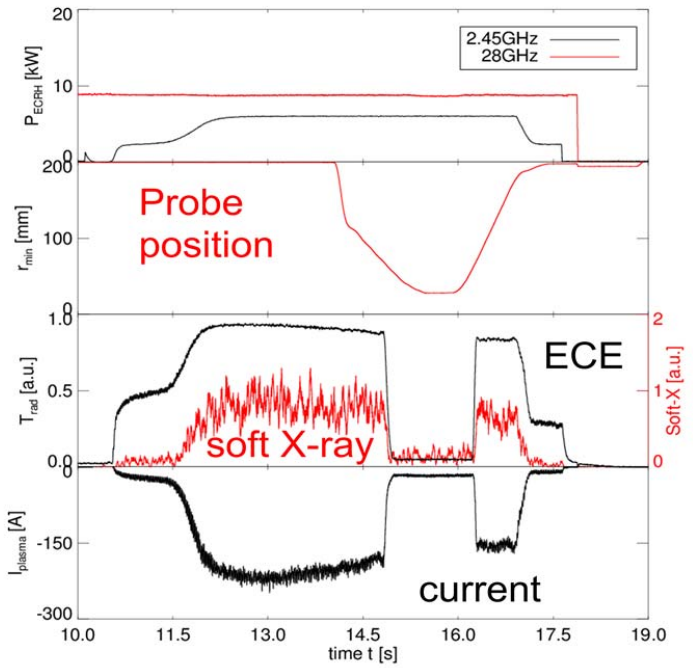

Figure 5: Time traces during probe insertion. Fast component is located within 20 mm at the plasma edge R=785 mm (see Fig 1).

The confinement time of the relativistic electrons was remarkably high and only limited by collisions with neutrals. After switching off the 2.45 GHz power, the decay time of the synchrotron radiation and the decay of the plasma current were found to decrease with neutral gas pressure (see **figure 6**). Values of up to 0.9 s were observed at the lowest achievable pressure demonstrating the superb particle confinement properties of the stellarator configuration. The PHA Sx-spectrum is shown in **figure 7.** It represents the bremsstrahlungs emission of the majority of the "run-away" electrons with medium energy by collisions with the plasma and neutral gas background. Up to 1 kA toroidal current was achieved by a heating power of 6 kW. Operation with higher heating power were prohibited due to the safety limit of γ-radiation dosis.

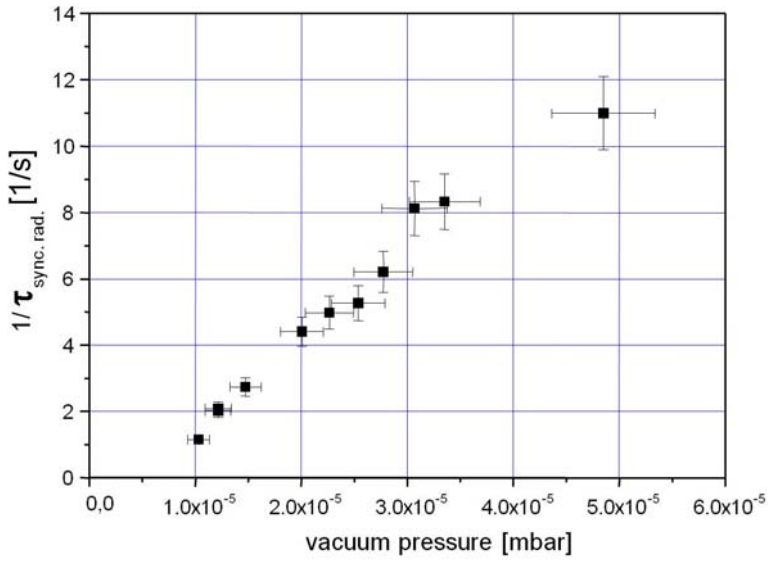

Figure 6: Inverse decay time of the synchrotron radiation after the power switch-off (see Fig.2 at 9.3 s) as a function of the He neutral gas pressure.

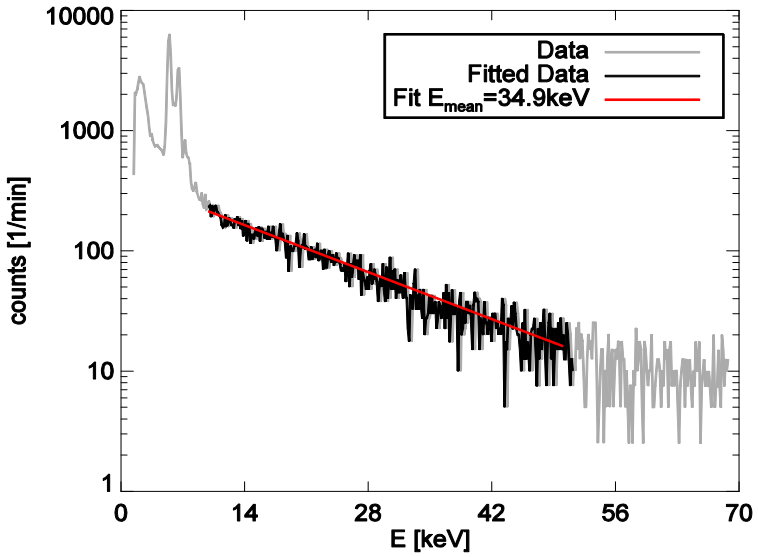

Fig. 7 SX-ray spectrum measured by a pulse height analyser.

5. Acceleration and heating

From these results we conclude that the plasma consists of two electron components: the bulk electrons, measured with the interferometer, and the relativistic electrons, whose existence is observed through the plasma net current, the synchrotron radiation, the x-rays and γ-rays. The number of bulk electrons, estimated from the average density and the plasma volume (0.1 m^3), was approximately 10^{17}. The lower limit for the number of relativistic electrons was estimated from the plasma current (typically 300 A) to be about 3×10^{13}, assuming that their parallel velocity is close to the velocity of light (*c*). An upper limit can be estimated from the change of the diamagnetic energy (1.7J), which was measured when the 2.45 GHz power was switched-off. Taking into account that the average energy per supra-thermal particle was at least 50 keV, which is the limit for an efficient interaction (see **figure 9**), the number is the 2.1×10^{14}. The acceleration mechanism is assumed to be based on a stochastic process taking place when the relativistic electrons pass the antenna RF-field similar to that described in [5]. The size of the antenna pattern close to its mouth is about half the vacuum wavelength. This means that electrons with a parallel velocity close to *c* can interact with the RF-field most efficiently. Whether there is an energy gain or loss depends on the phase relation between the electron position and the RF-field. Outside of this zone the electrons lose any phase information, since the time to encircle the torus ($\tau_{tor.\ orbit}$) is more than 40 times longer than the RF cycle (see **figure 8**) , the orbits are not closed (no rational rotation transform) and the electrons collide with the bulk electrons, ions and neutrals.

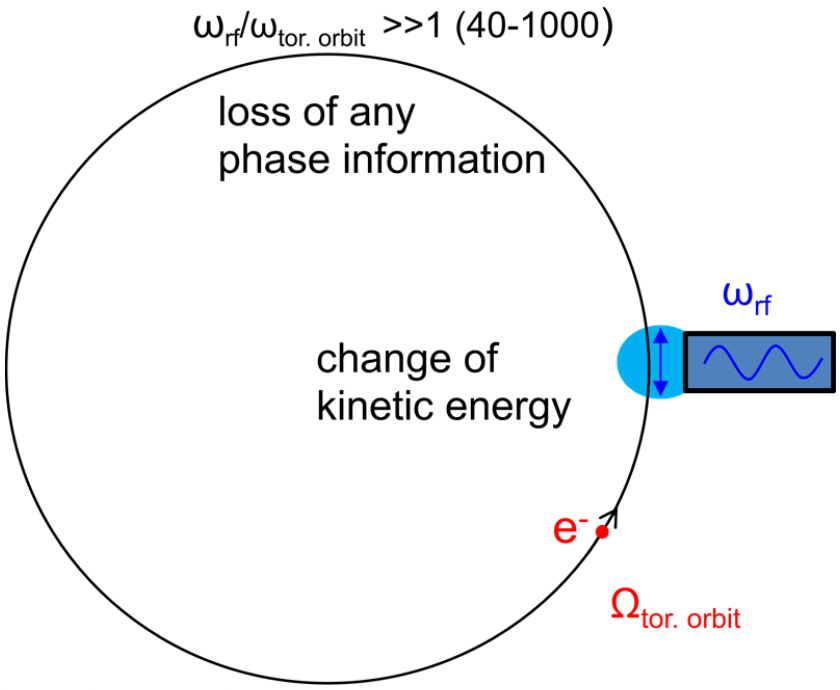

Figure 8: sketch of the acceleration mechanism.

For slower electrons this interaction becomes less effective because the E-field polarity changes sign several times during a passage through the RF-field and acceleration and de-acceleration compensate each other. The effect of many passages can be described as a diffusion process in energy space thus changing the distribution function of the electrons (EDF) in a statistical way. The corresponding random walk in energy space correspond to a diffusion coefficient, $D(E)=(<|\Delta E|>_E)^2/(2\tau_{tor.\ orbit})$ shown in **figure 9**, where $<|\Delta E|>_E$ is the average absolute energy step of an electron with kinetic energy E. It was calculated by solving the relativistic momentum equation of the electrons in the RF-field. The average was taken over the phase of the RF-field when the particles entered the field region. The electric field amplitude is calculated from the RF-antenna launched power (3 kW), taking into account reflection at the cut-off density. The resulting electric field E was 56kV/m with a Gaussian profile E Exp($-(x_{tor}/w)^2$) n the toroidal direction and a waste (2w) of 6.1 cm.

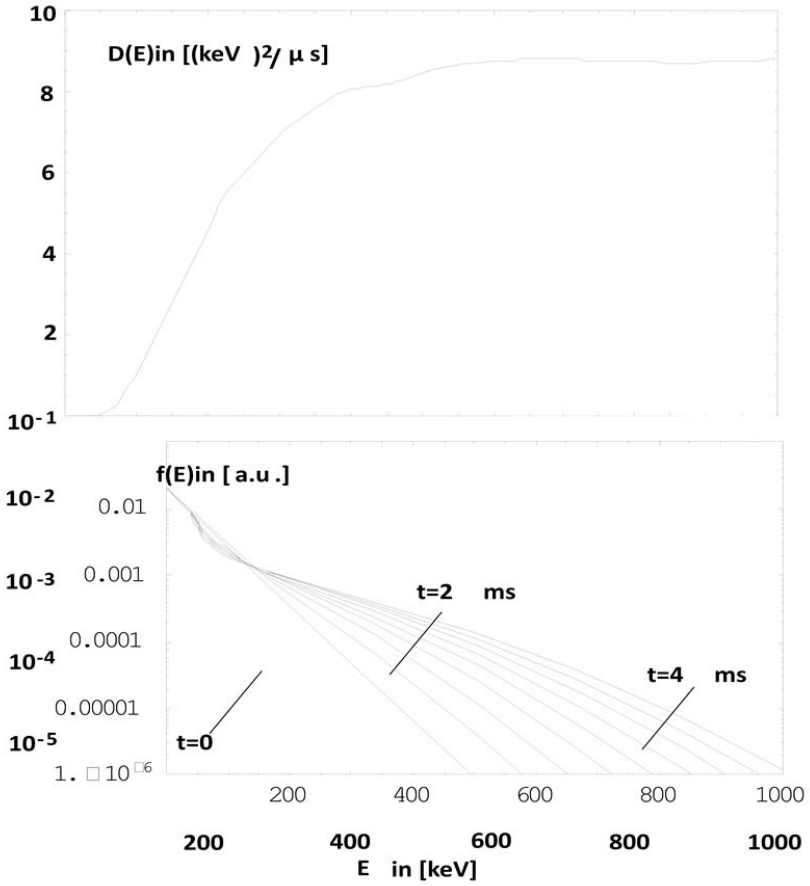

Figure 9 top: Diffusion coefficient D(E) vs. kin. Energy. bottom: Tail formation by diffusion of a Maxwellian EDF (T_e=50 keV) using D(E).

With this diffusion coefficient, the diffusion equation for the electron energy distribution function

$$\frac{\partial f}{\partial t} = \frac{\partial}{\partial E}\left(D(t,E)\frac{\partial f}{\partial E}\right) - \left(c_{Rutherford}(E^{-3/2}) - c_{inelastic}\right)f$$

was solved including two loss terms. The first ($c_{rutherford}$ $E^{-1.5}$) represets the coulomb collisions and the second cinelastic stays for energy independent inelastic collisions with neutrals. The simulation is initialized with a Maxwellian EDF and is over the plasma heating mechanism start-up. The steady state simulation requires many unknown parameters such as the pitch angle and energy distribution of secondary electrons and their orbits etc., so that an accurate and resilient solution would be difficult to achieve. Additionally, the diagnostics at WEGA are not able to measure the EDF with a sufficiently high precision to obtain a steady state solution. Fortunately, the characteristic time constants for the EDF relaxation is much longer (>20 ms see **figure 6**) than the diffusion time constant (<1 ms) and therefore these processes are separated in short pulse modulation experiments. The first result shows that only an EDF which already exhibits a significant electron component above 50 keV can interact with the RF-field. Therefore this kind of heating requires "seed" electrons for its start-up. In the experiment these were provided by the 28 GHz ECRH. Further, we calculated the average energy increase per time and particle. Multiplying this by the total number of the particles involved (3×10^{13} – 2.1×10^{14}), we get a lower and upper limit of the absorbed power,

$$P_{heat} = n_{fast}\frac{\partial}{\partial t}\int_0^\infty f(E)EdE$$

being of the order of 0.15-1 kW, which is a noticeable fraction of the input power of 3 kW. The interaction with the RF-field leads to tail formation in the EDF, which remarkably takes quite a long time (in the order of milliseconds as shown in Fig 8). The energy confinement time in ECRH-plasmas at WEGA is 0.5 ms for comparison. This result was corroborated in modulated power experiments (see **figure 10**). The RF-power of 3 kW was switched on for 1.5 ms and switched down to about 150 W for 15 ms repeatedly. The plasma signals were averaged over 10 modulation cycles in order to improve the signal to noise ratio. The time delay for the high energy tail ($\gamma > 5$) formation was deduced from the synchrotron radiation, which is emitted by those electrons only. The synchrotron radiation continues to increase after the power is switched down. This could be reproduced in the model when the remaining power of 150 W was introduced. The reason for this behaviour is that once a high energetic tail has been formed the small remaining power is sufficient to accelerate the electron to even higher energies. Since the synchrotron radiation strongly depends on the electron energy the radiation still increases. For the plasma current which is driven by all accelerated electrons the model predicts an immediate linear increase when the power is switched on. This was also observed in the experiment. The current started to decay immediately when the power was switched down. This is because the current is driven by all non-thermal electrons. In this case the large number of "low" energy electrons dominates the signal. If a loss term is introduced into the diffusion equation, the model reproduces the decay of the plasma current after switching down the power.

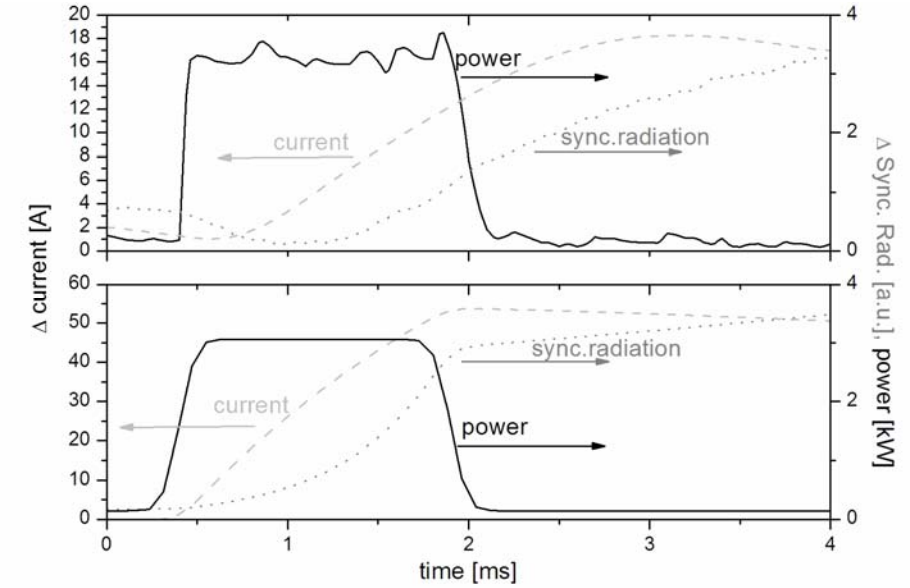

Figure 10: Comparison of experiment (top) and modelling (bottom). Time evolution of the plasma current (dashed) and synchrotron radiation (dots) when the heating power (solid) is modulated. The measured plasma current is delayed by the flux penetration time (0.3 ms) through the vacuum vessel wall

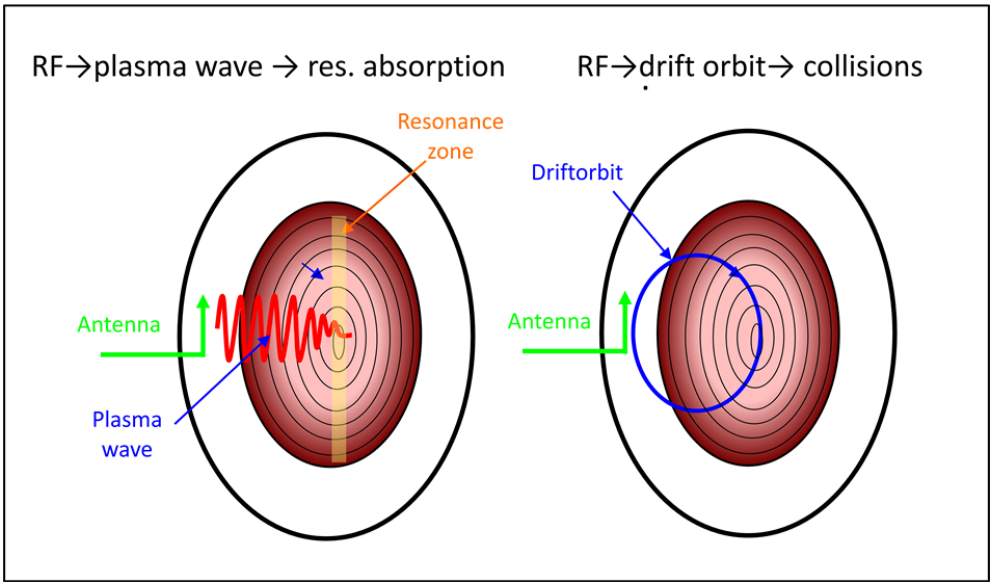

Figure 11: left RF plasma heating by wave excitation and resonant absorption. Right RF plasma heating by particle acceleration and drift orbits.

6. Discussion and conclusion

The acceleration process by stochastic interaction of relativistic electrons with the antenna field correctly explains the experimental results reported here. It reproduces the plasma current and high energy electron tail formation. It also explains why this scenario can only be started if there are previously existing relativistic electrons. In this experiment these electrons were produced by resonant ECRH, but other methods, like a finite loop voltage, could be similarly efficient [6]. The residence zone of the fast particles close to the antenna field was detected by a movable probe. Even though the fast electrons are accelerated at the plasma edge or even outside of the last closed flux surface, a low temperature bulk plasma could be sustained by this heating method. The fast electrons ionize and heat the central plasma by collisions. Simultaneously they compensate for losses due to absorption by in-vessel components (γ-emission) by generating new fast electrons in the collisional ionisation process. One might argue that the cross section for collision strongly decays with the particle energy. But this does not matter because the confinement time for the particle is in principle infinite. Therefore it will collide anyhow. There are two new physical effects in this heating process involved.

In contrast to standard RF-plasma heating methods, where the antenna excites plasma waves that transport the power to a resonance region in the plasma center, here the antenna accelerates fast particles (see **figure 11**). The large deviation of their particle drift orbits from the magnetic flux surfaces as shown in **figure 1** provides the energy transport from the antenna to the central plasma. This method neither necessitates a resonance in the plasma nor plasma wave excitation by the antenna. This heating and current drive mechanism is very robust. It can be applied over a wide range of magnetic field strengths and the plasma parameter at the antenna may vary over a large range. A similar heating mechanism using shifted drift orbits of ions was proposed for large tokamaks in [7].

Second, the stochastic acceleration here differs from the well known stochastic heating in RF capacitive discharges, where momentum transfer is accomplished by the oscillating sheath [8]. In case that the sheath is moving with $v_s=v_{0s}\cos\omega t$, the momentum change is $m_e v_{n+1}= m_e(v_n+2v_{0s}\cos\omega t)$ and the energy change is $1/2m_e(v_{n+1})^2=1/2m_e((v_n)^2+4(v_{0s}\cos\omega t)^2+4v_n v_{0s}\cos\omega t)$. Therefore there is an average energy gain of $m_e(v_{0s})^2$ for every single interaction. In our case it is the kinetic energy which is transferred. This process is symmetric for a single particle and the average energy gain is zero, but with the negative slope in the distribution function it generates positive overall energy transfer from the wave to the EDF.

7. References

[1] Fussmann G.; Physical Review E, 87, 013105(2013)
[2] Eicker H. und Krudewig W., Zeitschrift für Physik 188, 290-302 (1965)
[3] Podoba Y.Y., Laqua H.P., Warr G.B., Schubert M., Otte M., Marsen S., and Wagner F.: PRL **98,** 255003 (2007)
[4] Synchrotron radiation code at NIST: http:// physics.nist.gov/ MajResFac/SURF/SURF/schwinger.html
[5] Fuchs V. et al. Physica 14D (1985) 141-160
[6] Kobayashi S. et. al.; Nucl. Fus. 51 (2011) 062002 (4pp)
[7] Zehrfeld H. P., Fussmann B. and Green B. J.; Plasma Physics. Vol. 23, No. 5, pp. 473 to 489, 1981.
[8] Godyak V.A., *Sov. Phys. Tech. Phys.* **16**, No. 7, Jan. 1972